

DARK MATTER SEARCHES WITH IMAGING ATMOSPHERIC CHERENKOV TELESCOPES

E. MOULIN*

*CEA -Saclay, IRFU,
Gif-sur-Yvette, 91191, France
E-mail: emmanuel.moulin@cea.fr

The annihilations of WIMPs produce high energy gamma-rays in the final state. These high energy gamma-rays may be detected by imaging atmospheric Cherenkov telescopes (IACTs). Amongst the plausible targets are the Galactic Center, the centre of galaxy clusters, dwarf Spheroidal galaxies and substructures in Galactic haloes. I will review on the recent results from observations of ongoing IACTs.

Keywords: Dark matter, gamma-rays, Cherenkov telescopes

1. Introduction

Cosmological and astrophysical probes suggest that $\sim 23\%$ of the Universe is composed of non-baryonic dark matter (DM), commonly assumed to be in the form of Weakly Interacting Massive Particles (WIMPs) arising in extensions of the Standard Model of Particle Physics (for reviews see, e.g.^{1,2}). Amongst the most widely discussed DM candidates are the lightest neutralino in supersymmetric extensions of the Standard Model³ and the first excitation of the Kaluza-Klein bosons (LKP) in universal extra dimension theories.⁴⁻⁶

The annihilation of WIMP pairs can produce in the final state a continuum of gamma-rays whose flux extends up to the DM particle mass, from the hadronization and decay of the cascading annihilation products. In supersymmetric models, the gamma-ray spectrum from neutralino annihilation is not uniquely determined and the branching ratios (BRs) of the open annihilation channels are not determined since the DM particle field content is not known *a priori*. In contrast, in Kaluza-Klein scenarios where the lightest Kaluza-Klein particle (LKP) is the first KK mode of the hypercharge gauge boson, the BRs of the annihilation channels can be computed

given that the field content of the DM particle is known. The gamma-ray flux from annihilations of DM particles of mass m_{DM} accumulating in a spherical DM halo can be expressed in the form :

$$\frac{d\Phi(\Delta\Omega, E_\gamma)}{dE_\gamma} = \frac{1}{8\pi} \underbrace{\frac{\langle\sigma v\rangle}{m_{DM}^2} \frac{dN_\gamma}{dE_\gamma}}_{\text{Particle Physics}} \times \underbrace{\bar{J}(\Delta\Omega)\Delta\Omega}_{\text{Astrophysics}} \quad (1)$$

as a product of a particle physics component with an astrophysics component. The particle physics part contains $\langle\sigma v\rangle$, the velocity-weighted annihilation cross section, and dN_γ/dE_γ , the differential gamma-ray spectrum summed over the whole final states with their corresponding branching ratios. The astrophysical part corresponds to the line-of-sight-integrated squared density of the DM distribution J , averaged over the instrument solid angle $\Delta\Omega$ usually matching the angular resolution of the instrument :

$$J = \int_{l.o.s} \rho^2(r[s]) ds \quad \bar{J}(\Delta\Omega) = \frac{1}{\Delta\Omega} \int_{\Delta\Omega} PSF \times J d\Omega \quad (2)$$

where PSF stands for the point spread function of the instrument.

The annihilation rate being proportional to the square of the DM density integrated along the line of sight, regions with enhanced DM density are primary targets for indirect searches. Among them are the Galactic halo, external galaxies, galaxy clusters, substructures in galactic haloes, and the Galactic Center. We report here on recent results on dark matter searches with current IACTs such as H.E.S.S. and MAGIC, towards the Galactic Center, dwarf galaxies from the Local Group, Galactic globular clusters and DM mini-spikes around intermediate mass black holes (IMBHs).

2. The Galactic Centre

H.E.S.S. observations towards the Galactic Center have revealed a bright pointlike gamma-ray source, HESS J1745-290,⁷ coincident in position with the supermassive black hole Sgr A*, with a size lower than 15 pc. Diffuse emission along the Galactic plane has also been detected⁸ and correlates well with the mass density of molecular clouds from the Central Molecular Zone, as traced by CS emission.⁹ According to recent detailed studies,¹⁰ the source position is located at an angular distance of $7.3'' \pm 8.7''_{\text{stat.}} \pm 8.5''_{\text{syst.}}$ from Sgr A*. The pointing accuracy allows to discard the association of the very high energy (VHE) emission with the center of the radio emission of the supernova remnant Sgr A East but the association with the pulsar wind nebula G359.95-0.04 can not be ruled out. From 2004 data set, the

energy spectrum of the source is well fitted in the energy range 160 GeV - 30 TeV to a power-law spectrum $dN/dE \propto E^{-\Gamma}$ with a spectral index $\Gamma = 2.25 \pm 0.04_{\text{stat.}} \pm 0.1_{\text{sys.}}$. No deviation from a power-law is observed leading to an upper limit on the energy cut-off of 9 TeV (95% C.L.). The VHE emission from HESS J1745-290 does not show any significant periodicity or variability from 10 minutes to 1 year.¹⁰ Besides plausible astrophysical origins (see e.g.¹¹ and references therein), an alternative explanation is the annihilation of DM in the central cusp of our Galaxy. The spectrum of HESS J1745-290 shows no indication for gamma-ray lines. The observed gamma-ray flux may also result from secondaries of DM annihilation. The left hand side of Fig. 1 shows the H.E.S.S. spectrum extending up to masses of about 10 TeV, which requires large neutralino masses (>10 TeV). They are unnatural in phenomenological MSSM scenarios. The Kaluza-Klein models provide harder spectra which still significantly deviate from the measured one. Non minimal version of the MSSM may yield flatter spectrum with mixed 70% $b\bar{b}$ and 30% $\tau^+\tau^-$ final states. Even this scenario does not fit to the measured spectrum. The hypothesis that the spectrum measured by H.E.S.S. originates only from DM particle annihilations is highly disfavored.

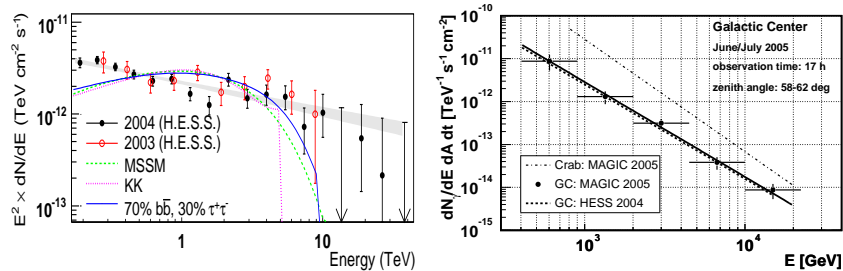


Fig. 1. Left : Spectral energy density $E^2 dN/dE$ of gamma-rays from HESS J1745-290 for 2003 (red empty circles) and 2004 (black filled circles) datasets of the H.E.S.S. observation of the Galactic Center. The shaded area shows the best power-law fit to the 2004 data points. The spectra expected from the annihilation of a MSSM-like 14 TeV neutralino (dashed green line), a 5 TeV KK DM particle (dotted pink line) and a 10 TeV DM particle annihilating into 70% $b\bar{b}$ and 30% $\tau^+\tau^-$ in final state (solid blue line) are presented. Right: Reconstructed VHE gamma-ray energy spectrum of the GC (statistical errors only) as measured by the MAGIC collaboration. The full line shows the result of a power-law fit to the data points. The dashed line shows the 2004 result of the HESS collaboration.¹³ The dot-dashed line shows the energy spectrum of the Crab nebula as measured by MAGIC.

The MAGIC observations were carried out towards the Galactic Centre since 2004 and revealed a strong emission. The observed excess in the direction of the GC has a significance of 7.3 standard deviations¹² and is compatible with a pointlike source. Large zenith observation angle ($\geq 60^\circ$) implies an energy threshold of ~ 400 GeV. The source position and the flux level are consistent with the measurement of HESS¹³ within errors. The right hand side of Fig. 1 shows the reconstructed VHE gamma-ray energy spectrum of the GC after the unfolding with the instrumental energy resolution. The differential flux can be well described by a power law of index $\Gamma = 2.2 \pm 0.2_{\text{stat.}} \pm 0.2_{\text{syst.}}$. The systematic error is estimated to be 35% in the flux level determination. The flux level is steady within errors in the time-scales explored within these observations, as well as in the two year time-span between the MAGIC and HESS observations. An interpretation in term of DM require a minimum value of mass higher than 10 TeV. Most probably, if DM signal exists is overcome by other astrophysical emitters.

3. Dwarf Galaxies from the Local Group

Dwarf spheroidal galaxies in the Local Group are considered as privileged targets for DM searches since they are among the most extreme DM-dominated environments. Measurements of roughly constant radial velocity dispersion of stars imply large mass-to-luminosity ratios. Nearby dwarfs are ideal astrophysical probes of the nature of DM as they usually consist of a stellar population with no hot or warm gas, no cosmic ray population and little dust. Indeed, these systems are expected to have a low intrinsic gamma-ray emission. This is in contrast with the Galactic Center where disentangling the dominant astrophysical signal from possible more exotic one is very challenging. Prior to the year 2000, the number of known satellites was eleven. With the Sloan Digital Sky Survey (SDSS), a population of ultra low-luminosity satellites has been unveiled, which roughly doubled the number of known satellites. Among them are Coma Berenices, Ursa Major II and Willman 1. IACTs have started observation campaigns on dwarf galaxies for a few years. Table 1 presents a possible list of the preferred targets for DM searches.

The star velocity dispersions in Draco reveal that this object is dominated by DM on all spatial scales and provide robust bounds on its DM profile, which thus decreases uncertainties on the astrophysical contribution to the gamma-ray flux. The MAGIC collaboration searched for a steady gamma-ray emission from the direction of Draco.¹⁷ The analysis energy threshold after cuts is 140 GeV. No significant excess is found.

Table 1. A tentative list of preferred dwarf galaxies.

Name	Distance ^a (kpc)	Luminosity ^a ($10^3 L_{\odot}$)	M/L ^b (M_{\odot}/L_{\odot})	Best positioned IACTs
Carina	101	430	40	HESS, CANGAROO
Coma Berenices	44	2.6	450	MAGIC, VERITAS
Draco	80	260	320	MAGIC, VERITAS
Fornax	138	15500	10	HESS, CANGAROO
Sculptor	79	2200	7	HESS, CANGAROO
Sagittarius	24	58000*	25	HESS, CANGAROO
Sextans	86	500	90	HESS, CANGAROO
Ursa Minor	66	290	580	MAGIC, VERITAS
Ursa Major II	32	2.8	1100	MAGIC, VERITAS
Willman 1	38	0.9	700	MAGIC, VERITAS

Note: ^aSee Ref. 14. ^bSee Ref. 15. *See Ref. 16.

For a power law with spectral index of 1.5, typical for a DM annihilation spectrum, and assuming a pointlike source, the 2σ upper limit is $\Phi(E > 140\text{GeV}) = 1.1 \times 10^{-11} \text{cm}^{-2}\text{s}^{-1}$. The measured flux upper limit is several orders of magnitude larger than predicted for the smooth DM distribution in mSUGRA models. The limit on the flux enhancement caused by high clumpy substructures or a black hole is around $O(10^3 - 10^9)$. The WHIPPLE collaboration has also observed Draco.¹⁸ Fig. 3 shows the 95% C.L. exclusion curve on σv . The upper limit is at the level of $10^{-22} \text{cm}^3\text{s}^{-1}$ for 1 TeV neutralino annihilating with BRs of 90% in $b\bar{b}$ and 10% in $\tau^+\tau^-$.

The Sagittarius (Sgr) dwarf galaxy, one of the nearest Galaxy satellites of the Local Group, has been observed by H.E.S.S. since 2006. The annihilation signal from Sgr is expected to come from a region of 1.5 pc, which is much smaller than the H.E.S.S. point spread function. Thus, a pointlike signal has been searched for. No significant gamma-ray excess is detected at the nominal target position. A 95% C.L. upper limit on the gamma-ray flux is derived: $\Phi_{\gamma}^{95\% \text{C.L.}}(E_{\gamma} > 250\text{GeV}) = 3.6 \times 10^{-12} \text{cm}^{-2}\text{s}^{-1}$, assuming a power-law spectrum of spectral index 2.2.¹⁹ A modelling of the Sgr DM halo has been carried out. Two models of the mass distribution for the DM halo have been studied: a cusped NFW profile and a cored isothermal profile, to encompass a large class of profiles. The cored profile has a small core radius due to a cusp in the luminous profile. The value of the line-of-sight-integrated squared density is then found to be larger for the cored profile than for the NFW profile (see Ref. 19 for more details). The left hand side of Fig. 2 presents the constraints on the velocity-weighted annihilation cross section σv for a cusped NFW and cored profiles in the solid

angle integration region $\Delta\Omega = 2 \times 10^{-5}$ sr, for neutralino DM. Predictions for SUSY models are displayed. For a cusped NFW profile, H.E.S.S. does not set severe constraints on σv . For a cored profile, due to a higher central density, stronger constraints are derived and some pMSSM models can be excluded in the upper part of the scanned region. Although the nature of Canis Major is still debated, HESS observed this object and results on Canis Major²⁰ are presented in Ref. 21.

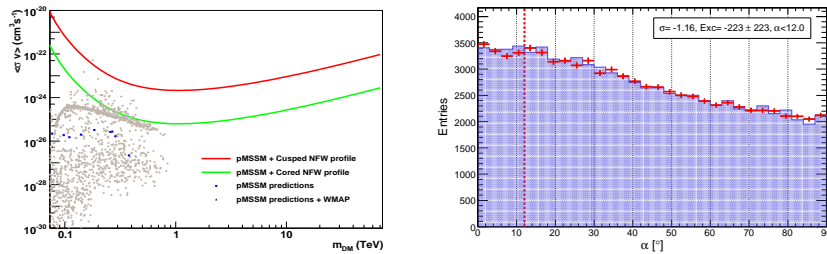


Fig. 2. Left: Upper limits at 95% C.L. on σv versus the neutralino mass for a cusped NFW and cored DM halo profile for Sgr. The predictions in pMSSM are also plotted with in addition those satisfying in addition the WMAP constraints on the cold DM density. Right: Willman 1 α -plot as seen by MAGIC in 15.5 hours above a fiducial energy threshold of 100 GeV. The red crosses represent the ON-data sample, the blue shaded region is the OFF-data sample normalized to the ON-data sample between $30^\circ - 80^\circ$. The vertical red dotted line represents the fiducial region $\alpha < 12^\circ$ where the signal is expected.

The recently discovered Willman 1 dwarf galaxy has been observed by MAGIC.²² Willman 1 has a total mass of $\sim 5 \times 10^5 M_\odot$, which is about an order of magnitude smaller than those of the least massive satellite galaxies previously known. This object has one of the highest mass-to-luminosity ratio. No significant gamma-ray excess beyond 100 GeV above the background was observed in 15.5 hours of observation of the sky region around Willman 1. This is shown in the right hand side of Fig. 2, where the " α -plot" is reported^a. The signal is searched with a cut slightly larger than for a pointlike source to take into account a possible source extension which makes a fiducial region to be $\alpha \leq 12^\circ$. Flux upper limits of the order of $10^{-12} \text{ cm}^{-2} \text{ s}^{-1}$ for benchmark mSUGRA models are obtained.²² Boost factors in flux of the order of 10^3 are required in the most optimistic scenarios, i.e. in

^aThe α -parameter is the angular distance between the shower image main axis and the line connecting the image barycenter and the camera center.

the funnel region or in region where the internal bremsstrahlung may play an important role. However, uncertainties on the DM distribution or the role of substructures may significantly reduce this boost.

4. Galactic Globular Clusters

Globular clusters are not believed to be DM-dominated objects. Their mass-to-luminosity ratios are well described by purely King profile which suggests no significant amount of DM. However, the formation of globular clusters fits in the hierarchical structure formation scenario in which globular clusters may have formed in DM overdensities. During their evolution, they may have hold some DM in their central region. M15 is a nearby galactic globular cluster with a core radius of 0.2 pc and a central density of $\sim 10^7 M_\odot \text{pc}^{-3}$. Even if the mass-to-light ratio of M15 does not suggest a significant component of DM, the compact and dense core of M15 does not prevent from looking for a hypothetical DM signal. The presence of stars and DM in globular clusters may lead to a DM enhancement in their inner part. This is usually treated with the adiabatic contraction model.²³

The Whipple collaboration observed M15 in 2003. The modelling of DM profile assuming adiabatic contraction of DM from an initial NFW distribution leads to an enhancement in the astrophysical factor of $\sim 10^2$ to

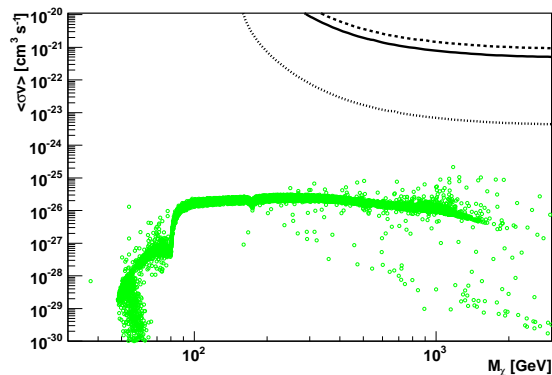


Fig. 3. Exclusion limit on σv as a function of the neutralino mass m_χ on M15 (dotted line) assuming an annihilation spectrum with 90% in $b\bar{b}$ and 10% in $\tau^+\tau^-$, and the NFW profile after adiabatic contraction. The solid line is the exclusion limit for Draco and the dashed line for Ursa Minor.

10^3 . Fig. 3 shows the exclusion curve on σv (dotted line) versus the neutralino mass assuming a NFW profile after adiabatic contraction.¹⁸ The limit reaches $\sim 10^{-24} \text{ cm}^3 \text{ s}^{-1}$ for TeV neutralinos.

5. Galaxy clusters

Astrophysical systems such as the VIRGO galaxy cluster²⁴ have been considered as target for DM annihilation searches. The elliptical galaxy M87 at the center of the VIRGO cluster has been observed by H.E.S.S. It is an active galaxy located at 16.3 Mpc which hosts a black hole of $3.2 \times 10^9 M_{\odot}$. From 2003 to 2006, H.E.S.S. detected a 13σ signal in 89 hour observation time at a location compatible with the nominal position of the nucleus of M87.²⁵ With the angular resolution of H.E.S.S., the VHE source is point-like, with an upper limit on the size of $3'$ at 99% confidence level. Given the distance of M87, this corresponds to a size of 13.7 kpc.

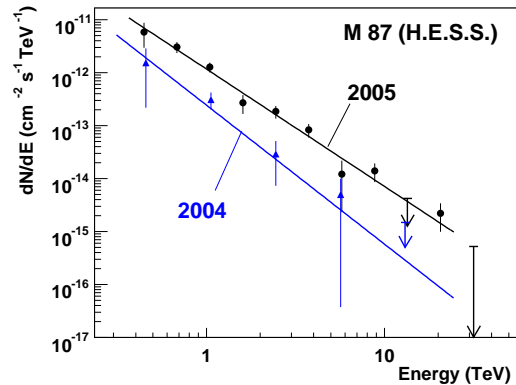


Fig. 4. Differential energy spectrum of M87 from ~ 400 GeV up to 10 TeV from 2004 and 2005 data. Corresponding fits to a power-law function dN/dE are plotted as solid lines. The data exhibit indices of $\Gamma = 2.62 \pm 0.35$ for 2004 and $\Gamma = 2.22 \pm 0.15$ for 2005.

Fig. 4 shows the energy spectrum for 2004 and 2005 data. Both data sets are well fitted to a power-law spectrum with spectral indices $\Gamma = 2.62 \pm 0.35$ (2004) and $\Gamma = 2.22 \pm 0.25$ (2005). The 2005 average flux is found to be higher by a factor ~ 5 to the average flux of 2004. The integrated flux above 730 GeV shows a yearly variability at the level of 3.2σ .²⁵ Variability at the day time scale has been observed in the 2005 data at the level of 4σ . This fast variability puts stringent constraints on the size of the VHE emission

region. The position centered on M87 nucleus excludes the center of the VIRGO cluster and outer radio regions of M87 as the gamma-ray emission region. The observed variability at the scale of ~ 2 days requires a compact emission region below $50R_s$, where $R_s \sim 10^{-15}$ cm is the Schwarzschild radius of the M87 supermassive black hole.²⁵ The short and long term temporal variability observed with H.E.S.S. excludes the bulk of the TeV gamma-ray signal to be of DM origin.

6. Galactic Substructures: the Case for IMBHs

Mini-spikes around Intermediate Mass Black Holes have been recently proposed as promising targets for indirect dark matter detection.²⁶ The growth of massive black holes inevitably affects the surrounding DM distribution. The profile of the final DM overdensity, called mini-spike, depends on the initial distribution of DM, but also on astrophysical processes such as gravitational scattering of stars and mergers. Ignoring astrophysical effects, and assuming adiabatic growth of the black hole, if one starts from a NFW profile, a spike with a power-law index $7/3$ is obtained, as relevant for the astrophysical formation scenario studied here characterized by black hole masses of $\sim 10^5 M_\odot$.²⁶ Mini-spikes might be detected as bright pointlike sources by current IACTs.

H.E.S.S. data collected between 2004 and 2007 during the Galactic plane survey have allowed to accurately map the Galactic plane between $\pm 3^\circ$ in galactic latitude and from -30° to 60° in galactic longitude with respect to the Galactic Center position. The study of the H.E.S.S. sensitivity in a large field of view to dark matter annihilations has been performed.²⁷ Fig. 5 shows the experimentally observed sensitivity map in the Galactic plane from Galactic longitudes $l=-30^\circ$ to $l=+60^\circ$ and Galactic latitudes $b=-3^\circ$ to $b=+3^\circ$, for a DM particle of 500 GeV mass annihilating into the 100% BR $b\bar{b}$ channel. The H.E.S.S. sensitivity depends strongly on the exposure time and acceptance maps which are related to the choice of the pointing positions. The flux sensitivity varies along the latitude and longitude due to inhomogeneous coverage of the Galactic plane. In the band between -2° and 2° in Galactic latitude, a DM annihilation flux sensitivity at the level of 10^{-12} $\text{cm}^{-2}\text{s}^{-1}$ is achieved for a 500 GeV DM particle annihilating in the $b\bar{b}$ channel. Deeper observations of the Galactic Center and at Galactic longitude of $\sim 20^\circ$ allow the flux sensitivity to be of $\sim 5 \times 10^{-13}$ $\text{cm}^{-2}\text{s}^{-1}$. For $b \geq 2^\circ$, the sensitivity is deteriorated due to a weaker effective exposure. For $b=0^\circ$ and $l=-0.5^\circ$, the flux sensitivity is $\sim 10^{-13}$ $\text{cm}^{-2}\text{s}^{-1}$ in $b\bar{b}$.

H.E.S.S. reached the required sensitivity to be able to test DM an-

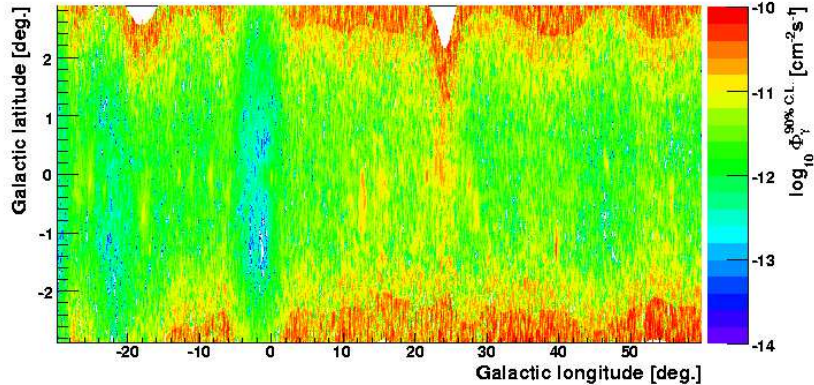


Fig. 5. H.E.S.S. sensitivity map in Galactic coordinates, i.e. 90% C.L. limit on the integrated gamma-ray flux above 100 GeV, for dark matter annihilation assuming a DM particle of mass $m_\chi = 500$ GeV and annihilation into the $b\bar{b}$ channel. The flux sensitivity is correlated to the exposure and acceptance maps. In the Galactic latitude band between -2° and 2° , the gamma-ray flux sensitivity reaches 10^{-12} $\text{cm}^{-2}\text{s}^{-1}$.

nihilations from mini-spikes in the context of one relatively favorable scenario for IMBH formation and adiabatic growth of the DM halo around the black hole (e.g. scenario B of Ref. 26). H.E.S.S. observations (2004-2006) of the Galactic plane allowed to discover more than 20 very high energy gamma-ray sources.²⁸ Some of them have been identified owing to their counterparts at other wavelengths, but almost half of the sources have no obvious counterpart and are still unidentified.²⁹ An accurate reconstruction of their energy spectra shows that all the spectra are consistent with a pure power-law, spanning up to two orders of magnitude in energy above the energy threshold. None of them exhibits an energy cutoff, characteristic of DM annihilation spectra, in the energy range from ~ 100 GeV up to 10 TeV. Furthermore, the detailed study of their morphology²⁹ shows that all the sources have an intrinsic spatial extension greater than ~ 5 arcminutes, while mini-spikes are expected to be pointlike sources for H.E.S.S. No IMBH candidate has been detected so far by H.E.S.S. within the survey range. Based on the absence of plausible IMBH candidates in the H.E.S.S. data, constraints are derived on the scenario B of Ref. 26 for neutralino or LKP annihilations, shown as upper limits on σv .²⁷ Fig. 6 shows the exclusion limit at the 90% C.L. on σv as a function of the neutralino mass. The neutralino is assumed to annihilate into $b\bar{b}$ and $\tau^+\tau^-$ with 100% BR,

respectively. Predictions for SUSY models are also displayed. The limits on

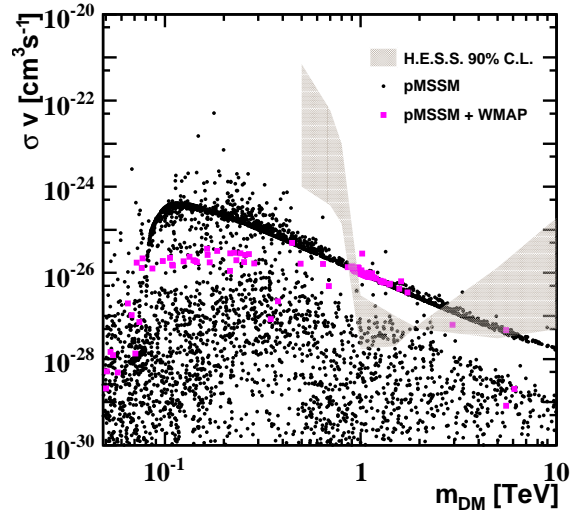


Fig. 6. Constraints on the IMBH gamma-ray production scenario for different neutralino parameters, shown as upper limits on σv as a function of the mass of the neutralino m_{DM} , but with a number of implicit assumptions about the IMBH initial mass function and halo profile (see Ref. 27 for details). For the scenario studied here, the probability of having no observable haloes in our Galaxy is 10% from Poisson statistics making these limits essentially 90% C. L. exclusion limits for this one particular (albeit optimistic) scenario (grey shaded area). The DM particle is assumed to be a neutralino annihilating into $b\bar{b}$ pairs or $\tau^+\tau^-$ pairs to encompass the softest and hardest annihilation spectra. The limit is derived from the H.E.S.S. flux sensitivity in the Galactic plane survey within the mini-spike scenario. SUSY models (black points) are plotted together with those satisfying the WMAP constraints on the DM particle relic density (magenta points).

σv are at the level of $10^{-28} \text{ cm}^3 \text{ s}^{-1}$ for the $b\bar{b}$ channel for neutralino masses in the TeV energy range. Limits are obtained one mini-spike scenario and constrain on the entire gamma-ray production scenario.

7. Conclusion

Dark matter searches will continue and searches with the phases 2 of H.E.S.S. and MAGIC will start soon. The phase 2 of H.E.S.S. will consist of a new large 28 m diameter telescope located at the center of the existing

array, and will allow to lower the analysis energy threshold down to less than 50 GeV. The installation of the second telescope on the MAGIC site will allow to perform more sensitive searches by the use of the stereoscopic mode. The upcoming generation of IACTs, the Cherenkov Telescope Array, is in the design phase. This array composed of several tens of telescopes will permit to significantly improve the performances on both targeted DM searches and wide-field-of-view DM searches.

References

1. G. Bertone, D. Hooper and J. Silk, *Phys. Rept.* **405**, 279 (2005).
2. L. Bergstrom, *Rept. Prog. Phys.* **63**, 793 (2000).
3. G. Jungman, M. Kamionkowski and K. Griest, *Phys. Rept.* **267**, 195 (1996)
4. T. Appelquist, H.-C. Cheng and B. A. Dobrescu, *Phys. Rev. D* **64**, 035002 (2001).
5. H. Cheng, J. Feng and K. Matchev, *Phys. Rev. Lett.* **89**, 211301 (2002).
6. G. Servant and T. Tait, *Nucl. Phys. B* **650**, 391 (2003).
7. F. Aharonian *et al.* [H.E.S.S. Collaboration], *Phys. Rev. Lett.* **97**, 221102 (2006) [Erratum-ibid. **97**, 249901 (2006)].
8. F. Aharonian *et al.* [H.E.S.S. Collaboration], *Nature* **439**, 695 (2006).
9. M. Tsuboi, H. Tsohihiro and N. Ukita, *Astrophys. J. Suppl.* **120** (2006) 675.
10. H.E.S.S. ICRC 2007 contributions, arXiv:0710.4057 [astro-ph].
11. F. Aharonian and A. Neronov, *Astrophys. J.* **619**, 306 (2005).
12. J. Albert *et al.* [MAGIC Collaboration], *Astrophys. J.* **638**, L101 (2006).
13. F. Aharonian *et al.* [HESS Collaboration], *Astron. Astrophys.* **425**, L13 (2004).
14. M. Mateo, *Ann. Rev. Astron. Astrophys.* **36**, 435 (1998).
15. J. D. Simon and M. Geha, *Astrophys. J.* **670**, 313 (2007).
16. A. Helmi and S. D. M. White, *Mon. Not. Roy. Astron. Soc.* **323**, 529 (2001).
17. J. Albert *et al.* [MAGIC Collaboration], *Astrophys. J.* **679**, 428 (2008).
18. M. Wood *et al.*, arXiv:0801.1708 [astro-ph].
19. F. Aharonian *et al.* [HESS Collaboration], *Astropart. Phys.* **29**, 55 (2008).
20. F. Aharonian *et al.* [HESS Collaboration], *Astrophys. J.* **691**, 175 (2009).
21. M. Vivier for the H.E.S.S. collaboration, *these proceedings*.
22. E. Aliu *et al.* [MAGIC Collaboration], arXiv:0810.3561 [astro-ph].
23. G. R. Blumenthal, S. M. Faber, R. Flores and J. R. Primack, *Astrophys. J.* **301**, 27 (1986).
24. E. A. Baltz, C. Briot, P. Salati, R. Taillet and J. Silk, *Phys. Rev. D* **61**, 023514 (2000).
25. D. Berge *et al.*, *Science* **314**, 1424 (2006).
26. G. Bertone, A. R. Zentner and J. Silk, *Phys. Rev. D* **72**, 103517 (2005).
27. F. Aharonian *et al.* [HESS Collaboration], *Phys. Rev. D* **78**, 072008 (2008).
28. F. Aharonian *et al.* [HESS Collaboration], *Astrophys. J.* **636**, 777 (2006).
29. F. Aharonian *et al.* [HESS Collaboration], *Astron. Astrophys.* **477**, 353 (2008).